ACS APPLIED MATERIALS & INTERFACES

Research Article

www.acsami.org

A Luminescent Cocaine Detection Platform Using a Split G-Quadruplex-Selective Iridium(III) Complex and a Three-Way DNA Junction Architecture

Dik-Lung Ma,*[,†,‡] Modi Wang,[†] Bingyong He,[†] Chao Yang,[§] Wanhe Wang,[†] and Chung-Hang Leung*[,§]

[†]Department of Chemistry, Hong Kong Baptist University, Hong Kong, China

[‡]Partner State Key Laboratory of Environmental and Biological Analysis, Hong Kong Baptist University, Hong Kong, China

[§]State Key Laboratory of Quality Research in Chinese Medicine, Institute of Chinese Medical Sciences, University of Macau, Macao, China

Supporting Information

ABSTRACT: In this study, a series of 10 in-house cyclometalated iridium(III) complexes bearing different auxiliary ligands were tested for their selectivity toward split G-quadruplex in order to construct a label-free switch-on cocaine detection platform employing a three-way junction architecture and a G-quadruplex motif as a signal output unit. Through two rounds of screening, we discovered that the iridium(III) complex 7 exhibited excellent selectivity toward the intermolecular G-quadruplex motif. A detection limit as low as 30 nM for cocaine can be achieved by this sensing approach with a linear relationship between luminescence intensity and cocaine concentration established from 30 to 300 nM. Furthermore, this sensing approach could detect cocaine in diluted oral fluid. We hope that our simple, signal-on, label-free oligonucleotide-based sensing method for cocaine using a three-way DNA junction architecture could act as a useful platform in bioanalytical research.

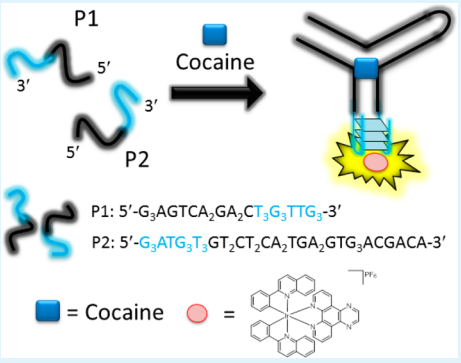

KEYWORDS: *iridium(III) complex, cocaine, three-way junction, label-free, G-quadruplex*

INTRODUCTION

Cocaine is an addictive drug and is the second-most used illegal substance in Europe and the United States.[1] Traditional methods for cocaine detection include chromatography techniques incorporate with mass spectrometry[2,3] and capillary electrophoresis (CE).[4] However, these instrumental analysis techniques generally require heavy, expensive instrumentation and labor-intensive sample preparation procedures and thus cannot be used for in-field sample evaluation. Commercial enzyme-linked immunosorbent assays (ELISA) for cocaine detection are also available but are limited to the use of expensive and thermally unstable antibodies.[5]

DNA three-way junctions are important building blocks in the construction of DNA architectures and dynamic assemblies.[6] It contains three double-helical arms that are connected at a junction point and form a branched structure. The formation of DNA three-way junctions is usually dynamic and acts as the simplified symbol for the replication fork and for viral DNA integration into the host DNA during retroviral replication.

Aptamers are oligonucleotides with a specific sequence that selectively recognize and bind to a target.[7,8] On the basis of the discovery of cocaine aptamer, several oligonucleotide-based cocaine detection methods with luminescent, colorimetric, and electrochemical signal outputs have been reported.[9−24] Upon specific binding with cocaine, the aptamers could fold into a typical three-way junction structure containing three stem loops connected at the junction point. The single cocaine aptamer chains, referred to as monolithic aptamers (MAs), can be cut into two pieces to obtain double-fragment aptamers (DFAs). Compared with MAs, the physical separation of two strands enhances flexibility and enables the possibility for probe modification in the development of new platforms for cocaine detection, while the use of shorter oligonucleotides could decrease the cost of the sensing platform for high throughput screening approach.

The G-quadruplex is generated from guanine-rich DNA and is stabilized by monovalent cations and Hoogsteen hydrogen bonding.[25−28] The rich structural diversity of G-quadruplex made it become a versatile signal transducing element for DNA-based sensing platforms.[23,24,29−44] One special kind of G-quadruplexes is called bimolecular or "split" G-quadruplexes, which are formed by the combination of two separate short, G-rich oligonucleotides. In this study, we combined the concepts of DNA aptamers, three-way junctions and split G-quadruplexes to construct a luminescent signal-on sensing platform for cocaine detection. The cocaine detection platform is described schematically in Scheme 1. P1 and P2 are designed

Received: May 8, 2015
Accepted: August 18, 2015
Published: August 18, 2015

DOI: 10.1021/acsami.5b05861
ACS Appl. Mater. Interfaces 2015, 7, 19060−19067

Scheme 1. Schematic Diagram of the Split G-Quadruplex-Based Luminescent Switch-on Detection Strategy for Cocaine Using the G-Quadruplex-Selective Iridium(Iii) Complex 7 and a Three-Way DNA Junction Architecture

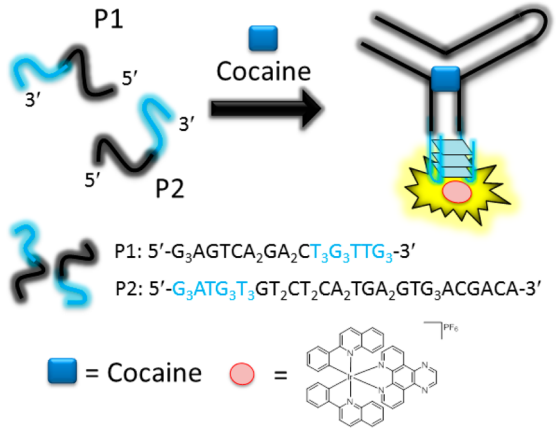

two DNA oligomers that each hold the split cocaine aptamer sequence in black and a split G-quadruplex sequence in blue, which allows the formation of split G-quadruplex structure when they get close to each other. First, P1 and P2 exist as a single-stranded (ssDNA) conformation and are far apart from each other. Thus, no split G-quadruplex motif could be formed, resulting in a weak luminescence signal. Upon addition of cocaine, the cocaine DFAs will bind to cocaine and form a three-way junction architecture. This allows the two split G-quadruplex-forming sequences getting close to each other, leading to the split G-quadruplex formation, which is subsequently identified by the G-quadruplex probe and generate a high luminescence signal.

Compared to traditional organic fluorophore, transition metal complexes can be synthesized easily with few steps,[45−47] while their photophysical properties and interactions with biomolecules can be readily tuned by variation of the coligands. Their relatively large Stokes shifts help to effectively decrease self-quenching, and the long emission lifetime of triplet metal-to-ligand charge transfer (^{3}MLCT) phosphorescence in the visible region allows their phosphorescence to be distinguished in highly fluorescent media through the use of time-resolved spectroscopy.[45,48−55] While iridium(III) complexes generally have longer lifetimes and higher quantum yield than ruthenium(II) complexes. Our group has previously developed a few iridium(III) complexes for unimolecular G-quadruplex DNA probe;[56−62] however, relatively less work has been conducted on probes that detect split G-quadruplexes.

EXPERIMENTAL SECTION

G-Quadruplex Fluorescent Intercalator Displacement (G4-FID) Assay. The FID assay was performed as previously described.[63]

Fluorescence Resonance Energy Transfer (FRET) Melting Assay. The FRET assay was performed according to literature.[43]

Synthesis. The following complexes were prepared according to (modified) literature methods.[46,50]

Cocaine Detection. P1, P2 (2.5 μL, each 100 μM) and cocaine was mixed in cocaine binding buffer (25 mM Tris-HCl containing 150 mM NaCl, pH 8.0). The mixture was incubated at 25 °C for 30 min. The prepared DNA mixture stock solution was diluted with cocaine binding buffer with 50 mM KCl to obtain a 0.5 μM DNA mixture solution in a cuvette, and then 1 μM of iridium(III) complex was added into the mixture. The mixture was then allowed to equilibrate at 25 °C for 10 min for emission measurement.

RESULTS AND DISCUSSION

Evaluvation of Iridium(III) Complexes as Intermolecular G-Quadruplex-Selective Probe. In this study, we first evaluated the emission response of four luminescent cyclometalated iridium(III) complexes (**1**−**4**, Figure 1) for their

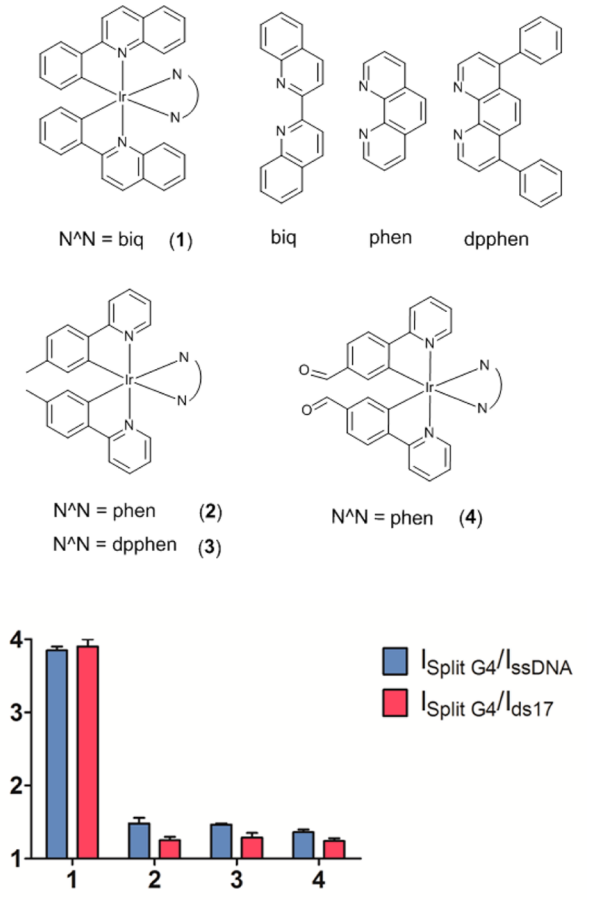

Figure 1. Diagrammatic bar array representation of the luminescence enhancement selectivity ratio of complexes **1**−**4** in the presence of split G-quadruplex over ssDNA or dsDNA.

ability to identify different kinds of DNA structure, including split G-quadruplex DNA, ssDNA, and double-stranded DNA (dsDNA, ds17). Among these four candidates, complex **1** incorporating the N^N ligand 2,2′-biquinoline (biq) and the C^N ligand 2-phenylquinoline (phq) showed best G-quadruplex selectivity (Figure 1), while showing small luminescence enhancements toward ssDNA and dsDNA. A fold enhancement ratio of *ca.* 3.8 and 3.9 was recorded for split G-quadruplex/ssDNA and split G-quadruplex/dsDNA, respectively. Based on the structure of complex **1**, we further designed and synthesized six derivatives of complex **1** (**5**−**10**, Figure 2). This library contains several favorable substructures of complex **1** which emerged as the top candidate in the first round of screening. Complexes **5**−**8** contain the same phq C^N ligand as complex **1**, but bear different N^N ligands with different biq derivatives. Encouragingly, the second round of screening revealed that the iridium(III) complex **7** has the best selectivity toward split G-quadruplex as it displayed the highest enhance-

DOI: 10.1021/acsami.5b05861
ACS Appl. Mater. Interfaces 2015, 7, 19060−19067

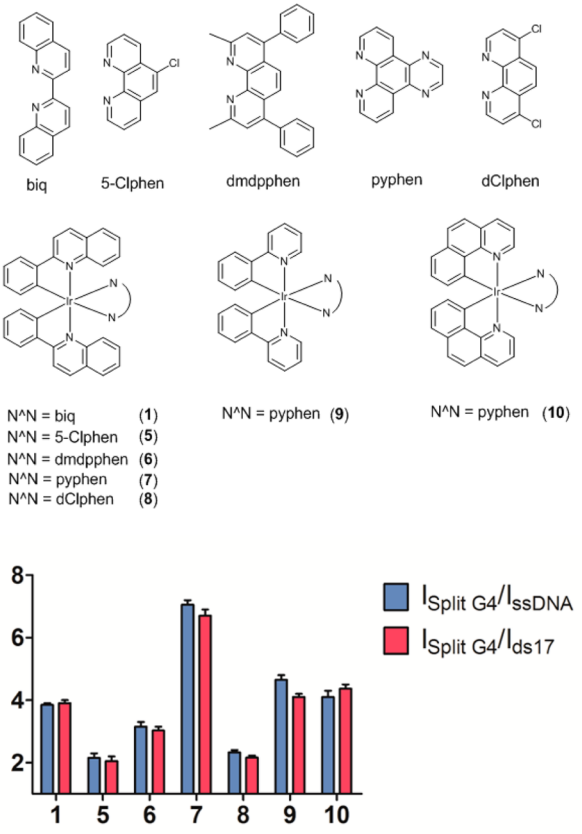

Figure 2. Diagrammatic bar array representation of the luminescence enhancement selectivity ratio of complexes **1** and **5**−**10** in the presence of split G-quadruplex over ssDNA or dsDNA.

ment ratio for split G-quadruplex over ssDNA and dsDNA (Figure 2).

Based on the screening data obtained, a basic structure−activity relationship can be deduced. Complex **7** contains the larger aromatic ring number of pyrazino[2,3-*f*][1,10]-phenanthroline(pyphen) ligand, compared with the biq ligand of the parent complex **1**, indicating that the size and shape of the N^N ligand may play a crucial role for split G-quadruplex binding. However, extremely bulky N^N ligands appear to reduce the split G-quadruplex binding, such as the two pendant phenyl groups linked to the phenanthroline scaffold for N^N^ ligand 2,9-dimethyl-4,7-diphenyl-1,10-phenanthroline (dmdpphen) in **6**. Complexes **5** and **8** which contain the 5-chloro-1,10-phenanthroline and 4,7-dichloro-1,10-phenanthroline ligand, showed the lowest luminescent enhancement in the second round of screening, suggesting that chlorine atom is undesirable for split G-quadruplex binding. Furthermore, complexes **9** and **10**, which contain the same pyphen ligand as **7** but vary in their C^N ligand, showed the relative low luminescent enhancement than **7**, indicating that complex **7**, which holds the phq C^N ligand and pyphen N^N ligand, displayed the best selectivity toward intermolecular G-quadruplex, with a luminescence enhancement ratio of *ca.* 7.1 and 6.7 over ssDNA and dsDNA (Figure 2).

To confirm the selectivity of iridium(III) complex **7** (Figure 3a) toward G-quadruplex DNA, we tested the luminescence signal of complex **7** upon addition of 17 different kinds of G-quadruplex sequences. Complex **7** displayed very weak luminescence in aqueous buffered solution. However, the luminescence intensity of complex **7** was significantly increased upon the addition of various G-quadruplex DNA sequences, especially the c-*kit* G-quadruplex DNA (Figure 3b). Complex **7** displayed a *ca.* 29.1-fold enhancement of luminescence signal upon the addition of 5 μM of c-*kit1* DNA, whereas *ca.* 20.4-fold enhancement was measured for c-*kit87up* DNA and a *ca.* 17.4-fold enhancement was measured for c-*kit2* DNA. Regarding to c-*myc* G-quadruplex DNA, complex **7** also shows a significant luminescent enhancement (*ca.* 20.5-fold for Myc48 and *ca.* 15.4-fold for c-*myc*). However, the luminescent response of complex **7** in the presence of human telomeric G-quadruplex DNA was not as high as for the aforementioned G-quadruplexes, with fold-changes of only 5−10 being observed. In contrast, no obvious luminescence change of complex **7** was measured in the presence of 5 μM of ssDNA and dsDNA. Therefore, these data indicate that complex **7** has selectivity for most G-quadruplex structures rather than ssDNA and dsDNA.

In line with other reported G-quadruplex selective probes, complex **7** displays very weak luminescence for thrombin binding aptamer (TBA) which only contain two G-quartet. One explanation is that TBA is more suitable for flat aromatic molecules than ribbon-like molecules. Moreover, complex **7** showed a relatively weak luminescence enhancement toward a G-quadruplex structure without loops (5′-TG_4T-3′). Therefore, we anticipate that complex **7** may bind outside the G-quartet and locate in the loop region. To prove this hypothesis, we evaluate the fold-enhancement of complex **7** in the presence of various G-quadruplex with different loop length. G-quadruplex sequences hold a 5′-side loop (5′-$G_3T_nG_3T_3G_3T_3G_3$-3′), a central loop (5′-$G_3T_3G_3T_nG_3T_3G_3$-3′) or a 3′-side loop (5′-$G_3T_3G_3T_3G_3T_nG_3$-3′), for which loop there are usually 1−12 nucleotides for loop length. The experimental data indicates that no matter the location of the loop, the luminescence enhancement of complex **7** increased with longer loop length until the maximum value (Figure S1). For the G-quadruplex structures with a 5′-side loop or central loop, complex **7** showed *ca.* 4-fold emission enhancement when the loop size was 1 or 2 nt. The luminescence of complex **7** increased uniformly to *ca.* 11-fold as the loop length was increased to 6 nt. With G-quadruplexes holding 3′-side loops, the fold enhancement of complex **7** increased from 4- to 10-fold as the loop length increased from 2 to 7 nt. These results outline that the property of the loop region could influence the binding between complex **7** and G-quadruplex and the G-quadruplex loop plays an essential role in the G-quadruplex-complex **7** binding.

To examine the selective G-quadruplex binding of complex **7**, we performed G-quadruplex fluorescent intercalator displacement (G4-FID). In principle, the additional G-quadruplex binding ligand will displace the thiazole orange (TO) from TO-G-quadruplex complex and decrease the luminescence of TO. While 2 μM of complex **7** displaces 50% of TO from TO-G-quadruplex assemble but only 20% displacement was observed for dsDNA upon addition of 5 μM complex **7** (Figure 3c). The result of FRET-melting assay is in line with this conclusion. Then 3 μM of complex **7** stabilizes the G-quadruplex DNA and increases the melting temperature (ΔT_m) for 5 °C but only about 1 °C for dsDNA (Figure 3d,e). Meanwhile, the enhanced melting temperature is nearly unchanged upon addition of 50-fold higher concentration of double stand or single strand DNA competitor (Figure 3f). In short, these results demonstrate that complex **7** selectively binds to G-quadruplex DNA but dsDNA or ssDNA.

DOI: 10.1021/acsami.5b05861
ACS Appl. Mater. Interfaces 2015, 7, 19060−19067

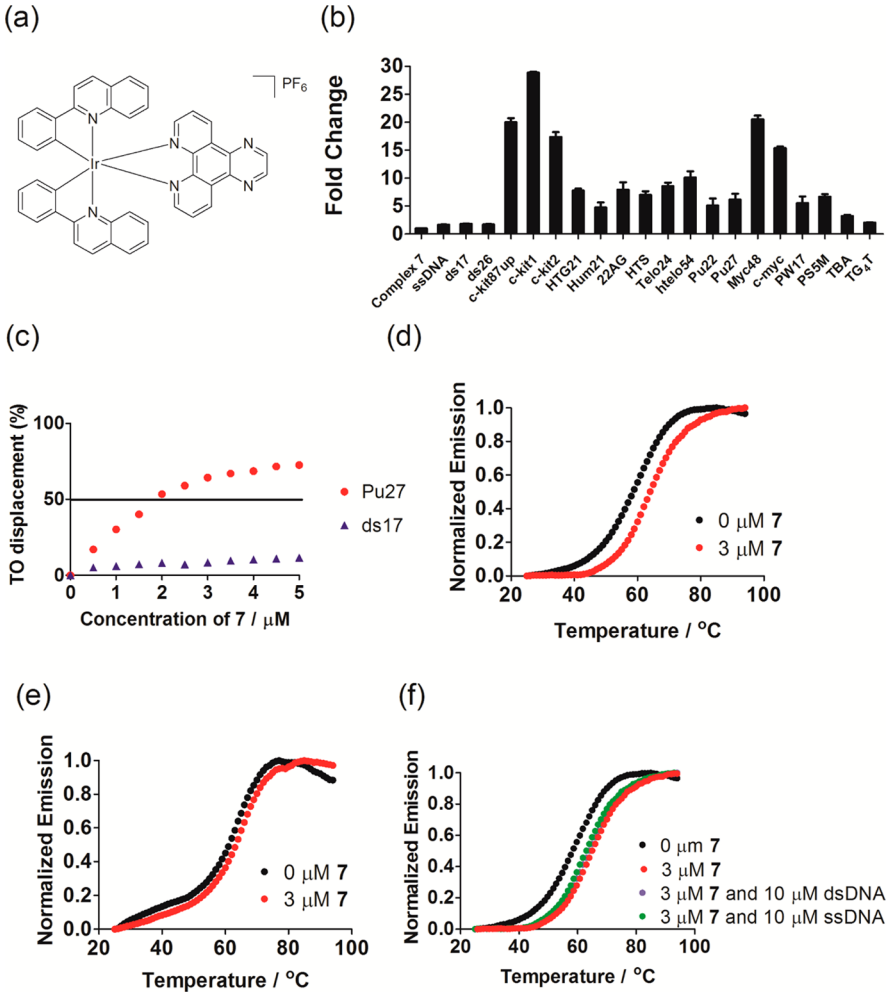

Figure 3. (a) Chemical structure of complex 7. (b) Diagrammatic bar array representation of the luminescence enhancement of complex 7 in the presence of ssDNA, dsDNA, and various kinds of G-quadruplex. (c) G4-FID titration curves of DNA duplex ds17 or G-quadruplex Pu27. (d) Melting profile of F21T G-quadruplex DNA (0.2 μM) in the absence and presence of 7 (3 μM). (e) Melting profile of F10T (0.2 μM) in the absence and presence of 7 (3 μM). (f) Melting profile of F21T G-quadruplex DNA (0.2 μM) in the absence and presence of 7 (3 μM) and ds26 (10 μM) or ssDNA (10 μM).

Luminescent Detection of Cocaine in Aqueous Solution. Encouraged by the superior seletivity of complex 7 toward G-quadruplex, we utilized complex 7 to design a sensing platform for cocaine detection in aqueous solution. We introduced 1 μM of cocaine into a solution containing 0.5 μM double-fragment cocaine aptamer DNA. After incubation at 25 °C for 30 min, complex 7 (1 μM) was added to the solution. Interestingly, we observed that complex 7 showed an enhanced luminescence signal with cocaine (Figure 4a). However, no luminescence enhancement of complex 7 was observed for the system lacking cocaine aptamer (Figure 4b), proving that the luminescence enhancement of complex 7 is not caused by direct interaction between complex 7 and cocaine. We envisage that the enhanced luminescence signal of complex 7 resulted from the specific binding of cocaine with its binding aptamer, which allows the formation of the three-way DNA junction architecture and subsequently the G-quadruplex motif that is recognized by 7. To demonstrate the mechanism of this assay, a few control experiments were conducted. Double-fragment cocaine aptamers containing mutant split G-quadruplex sequences ($P1_{m1}$ and $P2_{m1}$) were designed. The mutant sequences lack the important guanine bases that are essential in G-quadruplex formation. No significant change in the luminescence signal of complex 7 was displayed when mutant P1 and P2 were incubated with the target cocaine molecule (Figure 4c).

To further verify that the luminescence enhancement of complex 7 resulted from the recognition of complex 7 to split G-quadruplex induced by the binding between DFAs and cocaine at a three-way junction, we tried the sensing system with other DNA mutants, designated $P1_{m2}$ and $P2_{m2}$, which lack key bases in the aptamer sequences leading to a loss of binding affinity toward cocaine. The results showed that the luminescence signal of complex 7 was significantly decreased with those mutants (Figure 4c). Circular dichroism (CD) spectroscopy was further performed to demonstrate the proposed DNA switching in this platform. The characteristic G-quadruplex signals appeared with cocaine were consistent with literature (Figure 4d).[64] Thermal difference spectra (TDS) were also recorded to further validate the conformational change of the DNA. Without cocaine, the TDS only showed a broad positive peak at about 260 nm, which is the characteristic peak for dsDNA. With the addition of cocaine, a negative peak at about 290 nm was obtained, which is a typical characteristic for the G-quadruplex structure, thereby demonstrating the formation of G-quadruplex motif (Figure S2). These results

DOI: 10.1021/acsami.5b05861
ACS Appl. Mater. Interfaces 2015, 7, 19060−19067

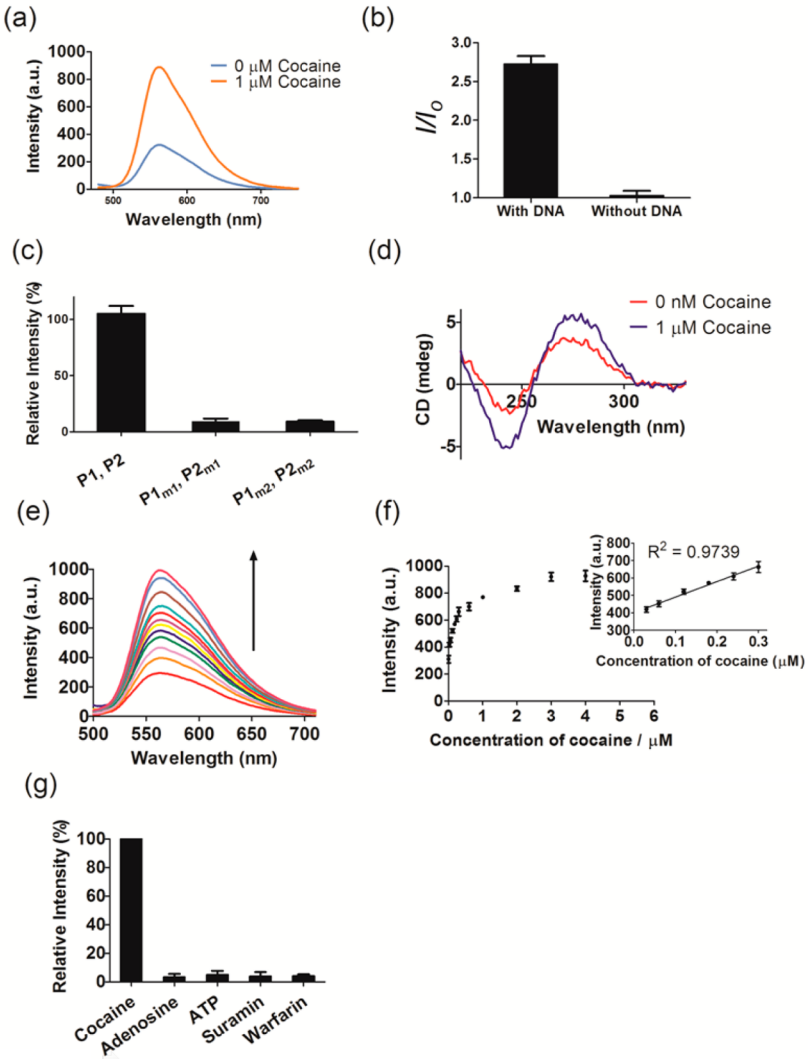

Figure 4. (a) Emission spectra of the system ([7] = 1 μM, [P1, P2] = 0.5 μM, [K^+] = 20 mM) in the presence or absence of cocaine (1 μM). (b) Luminescence enhancement of the system in response to cocaine (1 μM) in the presence or absence of P1, P2 (0.5 μM). (c) Relative luminescence response of the system using P1, P2, mutated $P1_{m1}$, $P2_{m1}$ or mutated $P1_{m2}$, $P2_{m2}$. (d) CD spectrum of 0.5 μM each of P1 and P2 in the absence and presence of 1 μM of cocaine. (e) Emission spectrum of the system in the presence of increasing concentrations of cocaine. (f) Linear plot of the change in luminescence intensity at λ = 560 nm vs cocaine concentration. (g) Relative luminescence intensity of the system in the presence of 1 μM cocaine or 5 μM other small molecules.

suggest that the enhanced luminescence signal of the system is highly related to the appearance of the G-quadruplex motif resulted from the binding between the DFAs and cocaine at a three-way junction architecture.

To further optimize the conditions of assay, we evaluated the effect of several parameters that may influence the performance of this sensing platform. First, it can be seen that the relative luminescence signal of the system was dependent on the concentration of complex 7 in solution, with a maximal intensity obtained at 1 μM of complex 7 (Figure S3a). Second, as potassium ions are crucial in the stabilization of the split G-quadruplex, the effect of KCl concentration on the luminescence signal of the platform was also investigated. We found that 20 mM of KCl provided a higher signal enhancement for the cocaine detection compared to 10, 50, or 100 mM of KCl (Figure S3b). Furthermore, we observed that the luminescence enhancement was the highest at a cocaine DFA concentration of 0.5 μM (Figure S3c). Finally, we also examined the effect of different asymmetrical "3 + 1" and symmetrical "2 + 2" split G-quadruplex designs on this cocaine sensing platform (Figure S3d). By using the previously optimized detection conditions, the P1 and P2 sequences showed the highest luminescence signal increase in the presence of cocaine among all six types of split G-quadruplexes. Under the optimized conditions, we tested the luminescence intensity of the detection platform upon addition of increasing concentrations of cocaine. The luminescence signal of complex 7 increased with the concentration of cocaine (Figure 4e). The system displayed a *ca.* 3.5-fold enhancement at [cocaine] = 4 μM, with a linear relationship established between luminescence intensity and cocaine concentrations of 30 and 300 nM (Figure 4f). Furthermore, the detection limit of this assay for cocaine was as low as 30 nM at a signal-to-noise ratio (S/N) of 3.

The selectivity of our assay for cocaine was examined by testing the luminescence response of the system toward four other small molecules (ATP, adenosine, warfarin, and suramin). Encouragingly, the luminescence output for cocaine was

DOI: 10.1021/acsami.5b05861
ACS Appl. Mater. Interfaces 2015, 7, 19060−19067

significantly higher than that for 5-fold higher concentrations of the other small molecules (Figure 4g). The selectivity of this platform for cocaine was further evaluvated by testing the signal output of the system to various planar compounds which could induce the structural switching of DNA, including ochratoxin A (OTA), thiazole orange (TO), protoporphyrin IX (PPIX), crystal violet (CV), thioflavin T (ThT) and adenosine triphosphate (ATP). Only weak luminescence response of the system were measured upon the addition of these compounds (Figure S4a). A competitive experiment was then conducted by adding these planar compounds to systems containing cocaine. The luminescent intensity of the system was closely unchanged in the presence of the other compounds (Figure S4b), indicating that this cocaine sensing platform could potentially be utilized to detect cocaine in a complicated matrix sample.

Application of Cocaine Detection Assay in Biological Samples. To test the performance in biological samples, we evaluated our sensing probe for the detection of cocaine under physiological conditions. A urine sample and an oral fluid sample were collected from a volunteer and diluted by Tris-HCl buffer. Increasing concentrations of cocaine were then spiked into the biological sample (0.5% v/v oral fluid and human urine). Our results showed that the luminescence intensity of system increased greatly as the concentration of cocaine was increased in both urine and oral fluid samples (Figure S5). Additionally, the assay showed acceptable performance even when more concentrated oral fluid (5% v/v) was used.

We also examine the performance of this assay to monitor the cocaine level in buffered solution containing 5 μM of ssDNA and dsDNA. The luminescence signal of the system exhibited a linear response with increasing concentrations of cocaine (Figure S5). These results indicate that the specificity of the 7/G-quadruplex interaction could be utilized for the effective detection of cocaine even in the presence of contaminating nucleic acids. These results suggest that our sensing platform could potentially be improved as a sensitive method for cocaine detection in the real application.

CONCLUSION

In summary, a series of 10 in-house cyclometalated iridium(III) complexes bearing different ligands were tested for their selectivity toward split G-quadruplex. We discovered that the iridium(III) complex 7 exhibited excellent selectivity toward split G-quadruplex DNA and thus could be applied in the development of a cocaine detection platform. In our approach, we combined the concepts of binding aptamers, three-way junctions and split G-quadruplexes to develop a label-free luminescent switch-on assay for the detection of cocaine. Compared with the previous methods in literatures utilizing fluorescently labeled nucleic acids, our "mix-and-measure" detection approach is easy, fast, and low cost and uses only unmodified oligonucleotides. A 30 nM detection limit for cocaine was obtained using complex 7, with a linear relationship from 30 to 300 nM. To allow for comparison with previous studies, we have summarized the detection limit, type of DNA used, and the practical application of other recently reported methods in Table S2. Some of these methods require modified DNA, which is much more expensive than the unmodified DNA oligonucleotides used in our system, though those methods do typically exhibit lower detection limits. A few of the assays could perform in real samples, such as diluted human serum and urine, which demonstrates the interest in potentially using these assays for the clinical testing of cocaine. The comparison table therefore highlights the fact that the sensitivity of our assay is comparable to previous studies, as well as the fact that our assay can perform in different kinds of biological samples, which has not been demonstrated for some of the previous assays. A more detailed discussion on recent oligonucleotide-based sensing platforms has been reviewed by Qu and co-workers.[65] We hope that our novel signal-on, label-free split G-quadruplex-based sensing method for cocaine could aid the study of clinical diagnosis and bioanalytical research.

ASSOCIATED CONTENT

Supporting Information

The Supporting Information is available free of charge on the ACS Publications website at DOI: 10.1021/acsami.5b05861.

Additoinal experimental details; DNA sequences used in this project; luminescence enhancement of complex 7 as a function of loop size; thermal difference spectrum; optimization data; relative luminescence intensity of the system in the presence of 1 μM cocaine or 1 μM other planar compounds and the competitive experiment; real sample detection; comparison of various detection methods of cocaine.(PDF)

AUTHOR INFORMATION

Corresponding Authors

*E-mail: edmondma@hkbu.edu.hk.

*E-mail: duncanleung@umac.mo.

Notes

The authors declare no competing financial interest.

ACKNOWLEDGMENTS

This work is supported by Hong Kong Baptist University (FRG2/14-15/004), Centre for Cancer and Inflammation Research, School of Chinese Medicine (CCIR-SCM, HKBU), the Health and Medical Research Fund (HMRF/13121482 and HMRF/14130522), the Research Grants Council (HKBU/201811, HKBU/204612, and HKBU/201913), the French National Research Agency/Research Grants Council Joint Research Scheme (A-HKBU201/12 - Oligoswitch), National Natural Science Foundation of China (21575121), Guangdong Province Natural Science Foundation (2015A030313816), Hong Kong Baptist University Century Club Sponsorship Scheme 2015, Interdisciplinary Research Matching Scheme (RC-IRMS/14-15/06), the Science and Technology Development Fund, Macao SAR (103/2012/A3 and 098/2014/A2), the University of Macau (MYRG091(Y3-L2)-ICMS12-LCH, MYRG2015-00137-ICMS-QRCM and MRG023/LCH/2013/ICMS).

REFERENCES

(1) Li, Y.; Qi, H.; Peng, Y.; Yang, J.; Zhang, C. Electrogenerated Chemiluminescence Aptamer-Based Biosensor for the Determination of Cocaine. *Electrochem. Commun.* **2007**, *9*, 2571−2575.

(2) Xia, Y.; Wang; Bartlett, M. G.; Solomon, H. M.; Busch, K. L. An LC−MS−MS Method for the Comprehensive Analysis of Cocaine and Cocaine Metabolites in Meconium. *Anal. Chem.* **2000**, *72*, 764−771.

(3) Kintz, P.; Mangin, P. Simultaneous Determination of Opiates, Cocaine and Major Metabolites of Cocaine in Human Hair by Gas Chromotography/Mass Spectrometry (GC/MS). *Forensic Sci. Int.* **1995**, *73*, 93−100.

(4) Lurie, I. S.; Klein, R. F. X.; Dal Cason, T. A.; LeBelle, M. J.; Brenneisen, R.; Weinberger, R. E. Chiral Resolution of Cationic Drugs

DOI: 10.1021/acsami.5b05861
ACS Appl. Mater. Interfaces 2015, 7, 19060−19067

of Forensic Interest by Capillary Electrophoresis with Mixtures of Neutral and Anionic Cyclodextrins. *Anal. Chem.* **1994**, *66*, 4019−4026.
(5) Pujol, M.-L.; Cirimele, V.; Tritsch, P. J.; Villain, M.; Kintz, P. Evaluation of the IDS One-Step ELISA Kits for the Detection of Illicit Drugs in Hair. *Forensic Sci. Int.* **2007**, *170*, 189−192.
(6) Ladbury, J. E.; Sturtevant, J. M.; Leontis, N. B. The Thermodynamics of Formation of a Three-Strand, DNA Three-Way Junction Complex. *Biochemistry* **1994**, *33*, 6828−6833.
(7) Ellington, A. D.; Szostak, J. W. In vitro Selection of RNA Molecules That Bind Specific Ligands. *Nature* **1990**, *346*, 818−822.
(8) Tuerk, C.; Gold, L. Systematic Evolution of Ligands by Exponential Enrichment: RNA Ligands to Bacteriophage T4 DNA Polymerase. *Science* **1990**, *249*, 505−510.
(9) Fang, X.; Tan, W. Aptamers Generated from Cell-SELEX for Molecular Medicine: A Chemical Biology Approach. *Acc. Chem. Res.* **2010**, *43*, 48−57.
(10) Iliuk, A. B.; Hu, L.; Tao, W. A. Aptamer in Bioanalytical Applications. *Anal. Chem.* **2011**, *83*, 4440−4452.
(11) Du, Y.; Li, B.; Wang, E. Fitting" Makes "Sensing" Simple: Label-Free Detection Strategies Based on Nucleic Acid Aptamers. *Acc. Chem. Res.* **2013**, *46*, 203−213.
(12) Li, Q.; Wang, Y.-D.; Shen, G.-L.; Tang, H.; Yu, R.-Q.; Jiang, J.-H. Split Aptamer Mediated Endonuclease Amplification for Small-Molecule Detection. *Chem. Commun.* **2015**, *51*, 4196−4199.
(13) Zhang, K.; Wang, K.; Zhu, X.; Zhang, J.; Xu, L.; Huang, B.; Xie, M. Label-free and Ultrasensitive Fluorescence Detection of Cocaine Based on a Strategy That Utilizes DNA-Templated Silver Nanoclusters and the Nicking Endonuclease-Assisted Signal Amplification Method. *Chem. Commun.* **2014**, *50*, 180−182.
(14) Zou, R.; Lou, X.; Ou, H.; Zhang, Y.; Wang, W.; Yuan, M.; Guan, M.; Luo, Z.; Liu, Y. Highly Specific Triple-Fragment Aptamer for Optical Detection of Cocaine. *RSC Adv.* **2012**, *2*, 4636−4638.
(15) Li, K.; Qin, W.; Li, F.; Zhao, X.; Jiang, B.; Wang, K.; Deng, S.; Fan, C.; Li, D. Nanoplasmonic Imaging of Latent Fingerprints and Identification of Cocaine. *Angew. Chem., Int. Ed.* **2013**, *52*, 11542−11545.
(16) Mokhtarzadeh, A.; Ezzati Nazhad Dolatabadi, J.; Abnous, K.; de la Guardia, M.; Ramezani, M. Nanomaterial-Based Cocaine Aptasensors. *Biosens. Bioelectron.* **2015**, *68*, 95−106.
(17) He, J.-L.; Yang, Y.-F.; Shen, G.-L.; Yu, R.-Q. Electrochemical Aptameric Sensor Based on the Klenow Fragment Polymerase Reaction for Cocaine Detection. *Biosens. Bioelectron.* **2011**, *26*, 4222−4226.
(18) Xie, S.-J.; Zhou, H.; Liu, D.; Shen, G.-L.; Yu, R.; Wu, Z.-S. In situ Amplification Signaling-Based Autonomous Aptameric Machine for the Sensitive Fluorescence Detection of Cocaine. *Biosens. Bioelectron.* **2013**, *44*, 95−100.
(19) Perrier, S.; Zhu, Z.; Fiore, E.; Ravelet, C.; Guieu, V.; Peyrin, E. Capillary Gel Electrophoresis-Coupled Aptamer Enzymatic Cleavage Protection Strategy for the Simultaneous Detection of Multiple Small Analytes. *Anal. Chem.* **2014**, *86*, 4233−4240.
(20) Roncancio, D.; Yu, H.; Xu, X.; Wu, S.; Liu, R.; Debord, J.; Lou, X.; Xiao, Y. A Label-Free Aptamer-Fluorophore Assembly for Rapid and Specific Detection of Cocaine in Biofluids. *Anal. Chem.* **2014**, *86*, 11100−11106.
(21) Liu, J.; Lu, Y. Fast Colorimetric Sensing of Adenosine and Cocaine Based on a General Sensor Design Involving Aptamers and Nanoparticles. *Angew. Chem.* **2006**, *118*, 96−100.
(22) Liu, J.; Mazumdar, D.; Lu, Y. A Simple and Sensitive "Dipstick" Test in Serum Based on Lateral Flow Separation of Aptamer-Linked Nanostructures. *Angew. Chem.* **2006**, *118*, 8123−8127.
(23) Xu, W.; Lu, Y. Label-Free Fluorescent Aptamer Sensor Based on Regulation of Malachite Green Fluorescence. *Anal. Chem.* **2010**, *82*, 574−578.
(24) Ma, D.-L.; He, H.-Z.; Leung, K.-H.; Zhong, H.-J.; Chan, D. S.-H.; Leung, C.-H. Label-Free Luminescent Oligonucleotide-Based Probes. *Chem. Soc. Rev.* **2013**, *42*, 3427−3440.
(25) Qureshi, M. H.; Ray, S.; Sewell, A. L.; Basu, S.; Balci, H. Replication Protein A Unfolds G-Quadruplex Structures with Varying Degrees of Efficiency. *J. Phys. Chem. B* **2012**, *116*, 5588−5594.
(26) Ray, S.; Qureshi; Mohammad, H.; Malcolm, D. W.; Budhathoki, J. B.; Çelik, U.; Balci, H. RPA-Mediated Unfolding of Systematically Varying G-Quadruplex Structures. *Biophys. J.* **2013**, *104*, 2235−2245.
(27) Ray, S.; Bandaria, J. N.; Qureshi, M. H.; Yildiz, A.; Balci, H. G-quadruplex Formation in Telomeres Enhances POT1/TPP1 Protection Against RPA Binding. *Proc. Natl. Acad. Sci. U. S. A.* **2014**, *111*, 2990−2995.
(28) Budhathoki, J. B.; Ray, S.; Urban, V.; Janscak, P.; Yodh, J. G.; Balci, H. RecQ-core of BLM Unfolds Telomeric G-quadruplex In the Absence of ATP. *Nucleic Acids Res.* **2014**, *42*, 11528−11545.
(29) Qu, K.; Zhao, C.; Ren, J.; Qu, X. Human telomeric G-quadruplex Formation and Highly Selective Fluorescence Detection of Toxic Strontium Ions. *Mol. BioSyst.* **2012**, *8*, 779−782.
(30) Zhu, Z.; Su, Y.; Li, J.; Li, D.; Zhang, J.; Song, S.; Zhao, Y.; Li, G.; Fan, C. Highly Sensitive Electrochemical Sensor for Mercury(II) Ions by Using a Mercury-Specific Oligonucleotide Probe and Gold Nanoparticle-Based Amplification. *Anal. Chem.* **2009**, *81*, 7660−7666.
(31) Zhao, C.; Wu, L.; Ren, J.; Qu, X. A Label-Free Fluorescent Turn-On Enzymatic Amplification Assay for DNA Detection Using Ligand-Responsive G-quadruplex Formation. *Chem. Commun.* **2011**, *47*, 5461−5463.
(32) Deng, S.; Cheng, L.; Lei, J.; Cheng, Y.; Huang, Y.; Ju, H. Label-Free Electrochemiluminescent Detection of DNA by Hybridization with a Molecular Beacon to Form Hemin/G-quadruplex Architecture for Signal Inhibition. *Nanoscale* **2013**, *5*, 5435−5441.
(33) Wen, Y.; Xu, Y.; Mao, X.; Wei, Y.; Song, H.; Chen, N.; Huang, Q.; Fan, C.; Li, D. DNAzyme-Based Rolling-Circle Amplification DNA Machine for Ultrasensitive Analysis of MicroRNA in Drosophila Larva. *Anal. Chem.* **2012**, *84*, 7664−7669.
(34) Xu, H.; Yang, Q.; Li, F.; Tang, L.; Gao, S.; Jiang, B.; Zhao, X.; Wang, L.; Fan, C. A Graphene-Based Platform for Fluorescent Detection of SNPs. *Analyst* **2013**, *138*, 2678−2682.
(35) Li, J.; Huang, Y.; Wang, D.; Song, B.; Li, Z.; Song, S.; Wang, L.; Jiang, B.; Zhao, X.; Yan, J.; Liu, R.; He, D.; Fan, C. A Power-Free Microfluidic Chip for SNP Genotyping Using Graphene Oxide and a DNA Intercalating Dye. *Chem. Commun.* **2013**, *49*, 3125−3127.
(36) Peng, Y.; Wang, X.; Xiao, Y.; Feng, L.; Zhao, C.; Ren, J.; Qu, X. i-Motif Quadruplex DNA-Based Biosensor for Distinguishing Single- and Multiwalled Carbon Nanotubes. *J. Am. Chem. Soc.* **2009**, *131*, 13813−13818.
(37) Chen, Z.; Lin, Y.; Zhao, C.; Ren, J.; Qu, X. Silver Metallization Engineered Conformational Switch of G-quadruplex for Fluorescence Turn-On Detection of Biothiols. *Chem. Commun.* **2012**, *48*, 11428−11430.
(38) Wang, C.; Wu, J.; Zong, C.; Ju, H.; Yan, F. Highly Sensitive Rapid Chemiluminescent Immunoassay Using the DNAzyme Label for Signal Amplification. *Analyst* **2011**, *136*, 4295−4300.
(39) Lin, D.; Wu, J.; Yan, F.; Deng, S.; Ju, H. Ultrasensitive Immunoassay of Protein Biomarker Based on Electrochemiluminescent Quenching of Quantum Dots by Hemin Bio-Bar-Coded Nanoparticle Tags. *Anal. Chem.* **2011**, *83*, 5214−5221.
(40) Yin, M.; Li, Z.; Liu, Z.; Ren, J.; Yang, X.; Qu, X. Photosensitizer-Incorporated G-quadruplex DNA-Functionalized Magnetofluorescent Nanoparticles for Targeted Magnetic Resonance/Fluorescence Multimodal Imaging and Subsequent Photodynamic Therapy of Cancer. *Chem. Commun.* **2012**, *48*, 6556−6558.
(41) Su, X.; Zhu, X.; Zhang, C.; Xiao, X.; Zhao, M. In Situ, Real-Time Monitoring of the 3′ to 5′ Exonucleases Secreted by Living Cells. *Anal. Chem.* **2012**, *84*, 5059−5065.
(42) Su, X.; Zhang, C.; Zhu, X.; Fang, S.; Weng, R.; Xiao, X.; Zhao, M. Simultaneous Fluorescence Imaging of the Activities of DNases and 3′ Exonucleases in Living Cells with Chimeric Oligonucleotide Probes. *Anal. Chem.* **2013**, *85*, 9939−9946.
(43) Leung, C.-H.; Zhong, H.-J.; He, H.-Z.; Lu, L.; Chan, D. S.-H.; Ma, D.-L. Luminescent Oligonucleotide-Based Detection of Enzymes Involved with DNA Repair. *Chem. Sci.* **2013**, *4*, 3781−3795.

DOI: 10.1021/acsami.5b05861
ACS Appl. Mater. Interfaces 2015, 7, 19060−19067

(44) Lin, Y.; Ren, J.; Qu, X. Catalytically Active Nanomaterials: A Promising Candidate for Artificial Enzymes. *Acc. Chem. Res.* **2014**, *47*, 1097−1105.
(45) Yang, Y.; Zhao, Q.; Feng, W.; Li, F. Luminescent Chemodosimeters for Bioimaging. *Chem. Rev.* **2013**, *113*, 192−270.
(46) Liu, J.; Liu, Y.; Liu, Q.; Li, C.; Sun, L.; Li, F. Iridium(III) Complex-Coated Nanosystem for Ratiometric Upconversion Luminescence Bioimaging of Cyanide Anions. *J. Am. Chem. Soc.* **2011**, *133*, 15276−15279.
(47) Metcalfe, C.; Thomas, J. A. Kinetically Inert Transition Metal Complexes That Reversibly Bind to DNA. *Chem. Soc. Rev.* **2003**, *32*, 215−224.
(48) Zhao, Q.; Huang, C.; Li, F. Phosphorescent Heavy-Metal Complexes for Bioimaging. *Chem. Soc. Rev.* **2011**, *40*, 2508−2524.
(49) Zhao, Q.; Li, F.; Huang, C. Phosphorescent Chemosensors Based on Heavy-Metal Complexes. *Chem. Soc. Rev.* **2010**, *39*, 3007−3030.
(50) Yu, M.; Zhao, Q.; Shi, L.; Li, F.; Zhou, Z.; Yang, H.; Yi, T.; Huang, C. Cationic Iridium(III) Complexes for Phosphorescence Staining in the Cytoplasm of Living Cells. *Chem. Commun.* **2008**, 2115−2117.
(51) Suntharalingam, K.; Łęczkowska, A.; Furrer, M. A.; Wu, Y.; Kuimova, M. K.; Therrien, B.; White, A. J. P.; Vilar, R. A Cyclometallated Platinum Complex as a Selective Optical Switch for Quadruplex DNA. *Chem. - Eur. J.* **2012**, *18*, 16277−16282.
(52) Georgiades, S. N.; Abd Karim, N. H.; Suntharalingam, K.; Vilar, R. Interaction of Metal Complexes with G-Quadruplex DNA. *Angew. Chem., Int. Ed.* **2010**, *49*, 4020−4034.
(53) Kitanovic, I.; Can, S.; Alborzinia, H.; Kitanovic, A.; Pierroz, V.; Leonidova, A.; Pinto, A.; Spingler, B.; Ferrari, S.; Molteni, R.; Steffen, A.; Metzler-Nolte, N.; Wölfl, S.; Gasser, G. A Deadly Organometallic Luminescent Probe: Anticancer Activity of a ReI Bisquinoline Complex. *Chem. - Eur. J.* **2014**, *20*, 2496−2507.
(54) Gasser, G.; Pinto, A.; Neumann, S.; Sosniak, A. M.; Seitz, M.; Merz, K.; Heumann, R.; Metzler-Nolte, N. Synthesis, Characterisation and Bioimaging of a Fluorescent Rhenium-Containing PNA Bioconjugate. *Dalton Trans.* **2012**, *41*, 2304−2313.
(55) Raszeja, L.; Maghnouj, A.; Hahn, S.; Metzler-Nolte, N. A Novel Organometallic ReI Complex with Favourable Properties for Bioimaging and Applicability in Solid-Phase Peptide Synthesis. *ChemBioChem* **2011**, *12*, 371−376.
(56) Ma, D.-L.; Chan, D. S.-H.; Leung, C.-H. Group 9 Organometallic Compounds for Therapeutic and Bioanalytical Applications. *Acc. Chem. Res.* **2014**, *47*, 3614−3631.
(57) He, H.-Z.; Chan, D. S.-H.; Leung, C.-H.; Ma, D.-L. A Highly Selective G-quadruplex-Based Luminescent Switch-On Probe for the Detection of Gene Deletion. *Chem. Commun.* **2012**, *48*, 9462−9464.
(58) Leung, K.-H.; He, H.-Z.; He, B.; Zhong, H.-J.; Lin, S.; Wang, Y.-T.; Ma, D.-L.; Leung, C.-H. Label-Free Luminescence Switch-On Detection of Hepatitis C Virus NS3 Helicase Activity Using a G-quadruplex-Selective Probe. *Chem. Sci.* **2015**, *6*, 2166−2171.
(59) Lu, L.; Chan, D. S.-H.; Kwong, D. W. J.; He, H.-Z.; Leung, C.-H.; Ma, D.-L. Detection of Nicking Endonuclease Activity Using a G-quadruplex-Selective Luminescent Switch-On Probe. *Chem. Sci.* **2014**, *5*, 4561−4568.
(60) Leung, C.-H.; Chan, D. S.-H.; He, H.-Z.; Cheng, Z.; Yang, H.; Ma, D.-L. Luminescent Detection of DNA-Binding Proteins. *Nucleic Acids Res.* **2012**, *40*, 941−955.
(61) Lin, S.; Gao, W.; Tian, Z.; Yang, C.; Lu, L.; Mergny, J.-L.; Leung, C.-H.; Ma, D.-L. Luminescence Switch-on Detection of Protein Tyrosine Kinase-7 Using a G-quadruplex-Selective Probe. *Chem. Sci.* **2015**, *6*, 4284−4290.
(62) Lu, L.; Wang, M.; Liu, L.-J.; Wong, C.-Y.; Leung, C.-H.; Ma, D.-L. A Luminescence Switch-On Probe for Terminal Deoxynucleotidyl Transferase (TdT) Activity Detection by Using an Iridium(iii)-Based i-motif Probe. *Chem. Commun.* **2015**, *51*, 9953−9956.
(63) Monchaud, D.; Allain, C.; Bertrand, H.; Smargiasso, N.; Rosu, F.; Gabelica, V.; De Cian, A.; Mergny, J. L.; Teulade-Fichou, M. P. Ligands Playing Musical Chairs with G-quadruplex DNA: A Rapid and Simple Displacement Assay for Identifying Selective G-quadruplex Binders. *Biochimie* **2008**, *90*, 1207−1223.
(64) Zhu, J.; Zhang, L.; Wang, E. Measurement of the Base Number of DNA Using a Special Calliper Made of a Split G-quadruplex. *Chem. Commun.* **2012**, *48*, 11990−11992.
(65) Wu, L.; Qu, X. Cancer Biomarker Detection: Recent Achievements and Challenges. *Chem. Soc. Rev.* **2015**, *44*, 2963−2997.

DOI: 10.1021/acsami.5b05861
ACS Appl. Mater. Interfaces 2015, 7, 19060−19067